

Second-order coherence of microwave photons emitted by a quantum point contact

Fabian Hassler and Daniel Otten

JARA-Institute for Quantum Information, RWTH Aachen University, D-52056 Aachen, Germany

(Dated: September 2015)

Shot-noise of electrons that are transmitted with probability T through a quantum point contact (biased at a voltage V_0) leads to a fluctuating current that in turn emits radiation in the microwave regime. By calculating the Fano factor F for the case where only a single channel contributes to the transport, it has been shown that the radiation produced at finite frequency ω_0 close to eV_0/\hbar and at low temperatures is nonclassical with sub-Poissonian statistics ($F < 1$). The origin of this effect is the fermionic nature of the electrons producing the radiation, which reduces the probability of simultaneous emission of two or more photons. However, the Fano factor, being a time-averaged quantity, offers only limited information about the system. Here, we calculate the second-order coherence $g^{(2)}(\tau)$ for this source of radiation. We show that due to the interference of two contributions, two photon processes (leading to bunching) are completely absent at zero temperature for $T = 50\%$. At low temperatures, we find a competition of the contribution due to Gaussian current-current fluctuations (leading to bunching) with the one due to non-Gaussian fluctuations (leading to antibunching). At slightly elevated temperatures, the non-Gaussian contribution becomes suppressed whereas the Gaussian contributions remain largely independent of temperature. We show that the competition of the two contributions leads to a nonmonotonic behavior of the second-order coherence as a function of time. As a result, $g^{(2)}(\tau)$ obtains a minimal value for times $\tau^* \simeq \omega_0^{-1}$. Close to this time, the second-order coherence remains below 1 at temperatures where the Fano factor is already above 1. We identify realistic experimental parameters that can be used to test the sub-Poissonian nature of the radiation.

PACS numbers: 73.50.Td, 42.50.Ar, 42.50.Lc, 73.23.-b

I. INTRODUCTION

In quantum optics, the degree of coherence plays a crucial role in characterizing different sources of radiation. In particular, the second-order coherence $g^{(2)}(\tau)$ is of central importance because it relates to the statistics of the radiation.¹ It can be shown that radiation sources whose fluctuations are independent of the optical phase such as lasers, thermal or chaotic light, all lead to $g^{(2)}(\tau) \geq 1$. Microscopically, this result can be interpreted as an effect due to the bunching of the photons. On the other hand, a radiation field with $g^{(2)}(\tau) < 1$ indicates that the radiation cannot be described in classical terms by a statistical superposition of coherent fields with different intensities. It is of fundamental interest to find and characterize radiation sources that produce nonclassical light. An important idea in this respect is to use the fermionic nature of electrons emitting the photons to imprint their antibunched statistics onto the radiation field. A prime example are single photon sources where a single electron in an excited state of an atom is used to emit a single photon.² An obvious question in this direction is whether there is a quantum limit to the classical light bulb where a resistive wire that is biased with a DC -voltage is employed to produce photons. This question has been affirmatively answered:³ the idea is to use a quantum point contact biased by a voltage V_0 . Single electrons are then transmitted stochastically (with probability T) through the barrier leading to current fluctuations. The photons produced by these current fluctuations are nonclassical provided the system is kept at low temperatures $\vartheta \ll eV_0/k_B$, with $e > 0$ the el-

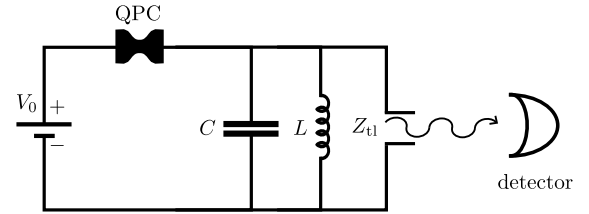


FIG. 1. Source (left part) and analyzer (right part) of the nonclassical radiation: A quantum point contact (QPC) is biased at a constant voltage V_0 and produces current-current fluctuations due to shot and thermal noise. These fluctuations are filtered by an LC -resonator and transmitted to the detector as electromagnetic-radiation via a transmission line with characteristic impedance Z_{tl} .

ementary charge and k_B the Boltzmann constant, such that the electron reservoirs are degenerate and bunching of the photons is suppressed. The suppression of bunching is achieved by two measures: firstly, only a single channel is allowed to contribute to the transport which requires the breaking of the spin-degeneracy in a magnetic field. Secondly, by engineering of the environment, the photons should be emitted preferentially at frequencies $\omega \geq eV_0/2\hbar$ such that each electron that carries an energy less than eV_0 emits at most a single photon.

The long-time properties of the radiation emitted by a quantum point contact, such as the Fano factor and even arbitrary cumulants of the photon counting statistics, have been obtained both at zero temperature³⁻⁵ and at finite temperatures⁶. Based on ideas of Ref. 7, a detector formed by two resonators at different frequen-

cies has been analyzed in details.⁵ Experimental progress has been impressive, resulting in the measurement of high-frequency shot-noise⁸ and the measurement of the two photon interference of photons emitted by a tunnel junction⁹. One of the last remaining challenges, the impedance matching of the wave-guides transporting the radiation from the quantum point contact to the amplifier that acts as a detector, has been recently resolved in employing superconducting circuits.^{10,11} Here, we want to study the second-order coherence $g^{(2)}(\tau)$, which is a time-resolved quantity and thus also carries information about the correlation time of the source. In particular, we show that the behavior of $g^{(2)}(\tau)$ as a function of the autocorrelation time τ is nonmonotonous with a minimum around $\tau^* \approx 5\omega_0^{-1}$. We highlight that a value $g^{(2)}(\tau^*) < 1$ can be obtained at temperatures where the radiation is already super-Poissonian.

The outline of the paper is as follows: In Sec. II, we present the experimental setup that is analyzed in the remainder of the paper. Sections III and IV provide the general results for the average photon rate as well as the photon-photon correlator that is directly linked to the second-order coherence. In Sec. V, we provide analytical results valid at zero temperature. We proceed by determining the critical temperatures below which the observation of nonclassical features in the radiation is possible in time-averaged quantities (Sec. VI) as well as the second-order coherence (Sec. VII). We conclude in Sec. VIII by identifying a set of realistic experimental parameters and provide results for the Fano factor and the second-order coherence for this case.

II. SETUP & MODEL

The setup we have in mind is shown in Fig. 1. The quantum point contact is assumed to be voltage-biased at a voltage V_0 and thus produces current noise $e^2 S(\omega) = \int dt \langle \langle I(0)I(t) \rangle \rangle e^{i\omega t}$ at frequency ω where $I(t)$ denotes the current through the quantum point contact and $\langle \langle \cdot \rangle \rangle$ indicates a cumulant. In the following, we assume that only a single channel with an energy-independent transmission probability $0 \leq T \leq 1$ contributes to the transport as the nonclassical signatures of the radiation are absent two or more channels.¹²

The source of current noise is embedded in an electromagnetic environment formed by an LC -resonator and a wide-band transmission line in parallel. The LC -resonator is characterized by the resonance frequency $\omega_0 = (LC)^{-1/2}$ and the characteristic impedance $Z_0 = (L/C)^{1/2}$, which is the ratio of the voltage to the current in the LC -resonator at the resonance frequency. As we want to treat the quantum point contact with impedance $2\pi\hbar/e^2T$ to be biased by a constant voltage, we have to assume that the impedance of the environment is small compared to the impedance of the quantum point contact, that is $G_Q Z_0 \ll 1$ with $G_Q = e^2/2\pi\hbar$.¹³ The transmission line introduces both damping as well as a slight

shift of the resonant frequency. The latter can be incorporated in a redefinition of ω_0 . The only relevant contribution of the impedance of the transmission line is its real part $Z_{tl}(\omega \approx \omega_0) = Z_0\omega_0/\gamma$ that we will parameterize by the rate γ whose meaning will be made clear below.

As the inductance, capacitance, and transmission line form a parallel circuit, the total impedance $Z_\omega = V_\omega/I_\omega$, relating the current $I(t) = \int (d\omega/2\pi) I_\omega e^{-i\omega t}$ through the quantum point contact to the voltage $V(t)$ across the LC -resonator, is given by

$$Z_\omega = \frac{Z_0\omega_0\omega}{i(\omega_0^2 - \omega^2) + \gamma\omega}. \quad (1)$$

As described in the introduction, the density of states for photons in the environment should be large for photons with frequency larger than $eV_0/2\hbar$. In order to achieve that, we have to require that $\gamma \lesssim eV_0/2\hbar$ and $\omega_0 \gtrsim eV_0/\hbar$. We have found that the optimal value of ω_0 is close to eV_0/\hbar , especially at temperatures close to the critical temperature. In order to keep the number of parameters manageable, we thus present only results for the resonant condition $\hbar\omega_0 = eV_0$ in the following (except for Fig. 7).

For positive frequencies (emission), the impedance is well-approximated by the form

$$\tilde{Z}_\omega = \frac{Z_0\omega_0}{2i(\omega_0 - \omega) + \gamma} \quad (2)$$

that corresponds to the response of an oscillator at frequency ω_0 with quality factor $Q = \omega_0/\gamma$. In particular, the rate γ describes the loss of photons from the cavity into the transmission line.¹⁴ Note that the total impedance on resonance $Z_{\omega_0} = QZ_0$ is a factor Q larger than the characteristic impedance of the resonator.

In a next step, we want to find an expression for the rate of photons $n(t)$ that are emitted at time t into the transmission line as those photons will be subsequently detected in the amplifier positioned at the other end. The photon number $dn(t) = P_\omega(t)d\omega/2\pi\hbar\omega$ in the frequency interval $[\omega, \omega + d\omega]$ is given by the power loss $P_\omega(t) = \text{Re}(Z_\omega^{-1}) \int d\delta V(t - \delta/2)V(t + \delta/2)e^{i\omega\delta}$ at this frequency measured in units of the photon energy $\hbar\omega$. Expressing the voltage $V_\omega = Z_\omega I_\omega$ via the current, we arrive at the important result

$$n(t) = \iint \frac{d\omega d\nu}{2\pi e^2} \alpha_\omega Z_{\omega+\nu/2}^* Z_{\omega-\nu/2} I_{\omega+\nu/2}^- I_{\omega-\nu/2}^+ e^{i\nu t} \quad (3)$$

with $\alpha_\omega = G_Q/Z_0Q\omega$, $I_\omega^+ = I_\omega\Theta(\omega)$ the current projected on the positive frequency contributions, and $I_\omega^- = (I_\omega^+)^\dagger$;¹⁵ here and below $\Theta(x)$ denotes the unit-step function. Positive frequency in this context corresponds to photon emission processes where energy from the electronic system is converted into photons. Note that in the limit of large quality factors $Q \gg 1$ when Z_ω is well-approximated by \tilde{Z}_ω , the photons are solely emitted at

the frequency ω_0 such that α_ω can be approximated by $\tilde{\alpha}_\omega = G_Q/Z_0 Q\omega_0$, which is independent of ω .

Below, the current $I(t)$ will be promoted to an operator and the usual normal-ordering prescription of photon counting denoted by colons will be assumed which implies that the ‘+’ operators are positioned to the right of the ‘-’ operators, with the ‘+’ operators being time-ordered, and the ‘-’ operators anti-time-ordered among themselves.¹⁶ Using this notation, the main task of this paper is the evaluation of the second-order coherence defined as

$$g^{(2)}(\tau) = \frac{\langle :n(\tau)n(0): \rangle}{\langle n \rangle^2}. \quad (4)$$

The current through the quantum point contact is the source of the radiation that is emitted in the transmission line. It can be evaluated using the conventional Landauer-Büttiker approach of transport. We model the quantum point contact by two electronic reservoirs, one to the left and one to the right of the constriction. The current operator at frequency ω has the explicit form $I_\omega = I_{\text{out},\omega} - I_{\text{in},\omega}$ with

$$I_{\text{in},\omega} = e \int d\epsilon c_{R,\epsilon}^\dagger c_{R,\epsilon+\omega}, \quad I_{\text{out},\omega} = e \int d\epsilon d_\epsilon^\dagger d_{\epsilon+\omega}; \quad (5)$$

here, $d_\epsilon = T^{1/2}c_{L,\epsilon} - R^{1/2}c_{R,\epsilon}$ with the reflection probability is given by $R = 1 - T$ due to unitarity. The electronic states in the reservoirs are described by fermionic operators $c_{x,\epsilon}$ that fulfill the canonical anticommutation relations $\{c_{x,\epsilon}, c_{x',\epsilon'}\} = 0$ and $\{c_{x,\epsilon}, c_{x',\epsilon'}^\dagger\} = \delta_{xx'}\delta(\epsilon - \epsilon')$ with $x, x' \in \{L, R\}$. The states are assumed to be in (local) equilibrium and thus occupied according to the Fermi-Dirac distribution $\langle c_{x,\epsilon}^\dagger c_{x',\epsilon'} \rangle = \delta_{xx'} f_x(\epsilon)\delta(\epsilon - \epsilon')$ with

$$f_x(\epsilon) = (\exp[(\hbar\epsilon - \mu_x)/k_B\vartheta] + 1)^{-1}. \quad (6)$$

In the following, we will measure the electronic energies with respect to the chemical potential of the right reservoir and thus set $\mu_R = 0$ and $\mu_L = eV_0$ (due to the voltage bias).

III. AVERAGE PHOTON RATE

The photon rate can be calculated by averaging the expression (3) over the distribution of the electrons. Due to the fact that the bias V_0 is constant, the state is stationary and as a result the average photon rate $\langle n(t) \rangle$ is independent of t . The photon rate assumes the simple form

$$\langle n \rangle = \int_0^\infty d\omega \alpha_\omega |Z_\omega|^2 S(\omega). \quad (7)$$

The current noise power $S(\omega)$ can be evaluated by employing Wick’s theorem yielding the result $S(\omega) =$

$S_{\text{ex}}(\omega) + S_{\text{th}}(\omega)$ with

$$\begin{aligned} S_{\text{ex}}(\omega) &= RT \int \frac{d\epsilon}{2\pi} \Delta(\epsilon + \omega) \Delta(\epsilon) \\ &= \frac{RT \operatorname{sh}(\frac{\hbar\omega_0}{2k_B\vartheta})}{4\pi \operatorname{sh}(\frac{\hbar\omega}{2k_B\vartheta})} \left(\frac{\omega_0 - \omega}{\operatorname{sh}[\frac{\hbar(\omega_0 - \omega)}{2k_B\vartheta}]} - \frac{\omega_0 + \omega}{\operatorname{sh}[\frac{\hbar(\omega_0 + \omega)}{2k_B\vartheta}]} \right) \end{aligned} \quad (8)$$

and

$$S_{\text{th}}(\omega) = T \int \frac{d\epsilon}{\pi} f_R(\epsilon + \omega) f_R(-\epsilon) = \frac{T\omega}{\pi(e^{\hbar\omega/k_B\vartheta} - 1)};$$

here, we have introduced the abbreviation $\Delta(\omega) = f_L(\omega) - f_R(\omega)$ for convenience. The term $S_{\text{th}}(\omega)$ in the expression for $S(\omega)$ describes the thermal noise whereas $S_{\text{ex}}(\omega)$ is the excess noise due to the application of a finite bias V_0 . At zero temperature, only the excess noise remains at positive frequencies. Note that at low temperatures and large quality factors, we may replace S , Z , and α in (7) by S_{ex} , \tilde{Z} , and $\tilde{\alpha}$ respectively. As a result, we obtain the approximate expression

$$\langle n \rangle = \int_0^\infty d\omega \frac{G_Q Z_0 \gamma S_{\text{ex}}(\omega)}{4(\omega_0 - \omega)^2 + \gamma^2}. \quad (9)$$

Figure 2 shows a comparison of the photon rate, Eq. (7), with the approximation (9).

The photon rate depends on the three energy scales eV_0 , $\hbar\gamma$, and $k_B\vartheta$. We can evaluate $\langle n \rangle$ in the different relevant limits and obtain the following approximations

$$\langle n \rangle \approx \frac{RTG_Q Z_0}{8\pi} \begin{cases} 2\pi k_B\vartheta/\hbar, & \hbar\gamma \ll k_B\vartheta \ll eV_0, \\ \gamma \ln(2Q), & k_B\vartheta \ll \hbar\gamma \ll eV_0. \end{cases} \quad (10)$$

Since γ denotes the rate at which photons are transferred from the LC -resonator to the transmission line, the number of photons in the cavity n_{cav} is given by $\langle n \rangle/\gamma \simeq RTG_Q Z_0 \max(1, 2\pi k_B\vartheta/\hbar\gamma)/8\pi$. As we are mainly interested in the low-temperature limit in the following, we use the abbreviation

$$n_{\text{cav}} = \frac{RTG_Q Z_0}{8\pi} \quad (11)$$

consistently.

IV. PHOTON-PHOTON CORRELATION

In order to obtain the second-order coherence, the task is to obtain the photon-photon correlation function $n^{(2)}(\tau) = \langle \langle :n(\tau)n(0): \rangle \rangle = \langle :n(\tau)n(0): \rangle - \langle n \rangle^2$. Given this correlation function, the second-order coherence follows via

$$g^{(2)}(\tau) = \frac{n^{(2)}(\tau)}{\langle n \rangle^2} + 1. \quad (12)$$

In particular, a negative correlation function $n^{(2)}(\tau)$ at some time τ is equivalent to having $g^{(2)}(\tau) < 1$

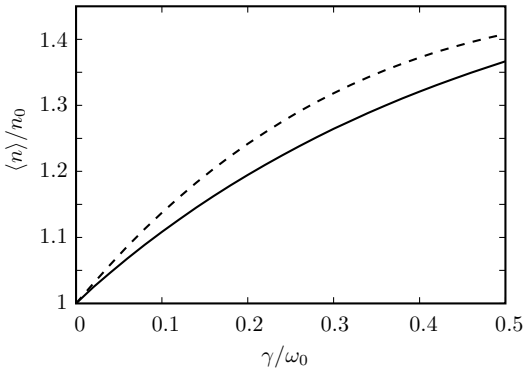


FIG. 2. Comparison of the photon rate of Eq. (7) (solid line) with the approximate expression Eq. (9) (dashed line) for $T = \frac{1}{2}$ and $k_B \vartheta / eV_0 = 0.1$ as a function of γ / ω_0 normalized to the value $n_0 = RTG_Q Z_0 k_B \vartheta / 4\hbar$ valid for $\gamma \rightarrow 0$.

and thus indicates nonclassical radiation. The prior work³⁻⁵ has been concentrated on obtaining zero frequency (long-time) results. In particular, the Fano factor $F = \int d\tau \langle \langle :n(\tau)n(0): \rangle \rangle / \langle n \rangle$ describing whether a source is more correlated ($F > 1$) or anticorrelated ($F < 1$) than a Poissonian source with $F = 1$ has been of central interest. The connection with $g^{(2)}$ is provided by¹⁷

$$F - 1 = \langle n \rangle \int d\tau [g^{(2)}(\tau) - 1] = \frac{N^{(2)}}{\langle n \rangle}. \quad (13)$$

where we have introduced the total number of correlated photons $N^{(2)} = \int d\tau n^{(2)}(\tau)$. A Fano factor with $F < 1$ is a clear indication that $g^{(2)}(\tau)$ is smaller than one for some τ . However, having the full information $g^{(2)}(\tau)$ available, it is possible to have $g^{(2)}(\tau) < 1$ for some time $\tau = \tau^*$ even when $F \gtrsim 1$.

Obtaining the photon-photon correlation function $n^{(2)}(\tau)$ is more difficult than the average photon rate. The problem is that it involves the evaluation of a forth-order current correlators. We proceed with the insight of Ref. 4 that the normal-ordering of the current operators is equivalent to the *in-out*-ordering, *i.e.*, ordering I_{in}^- , I_{out}^- , I_{out}^+ , I_{in}^+ from left to right. The concrete ordering within a group of these operators does not matter, since $[I_{\text{in}}(t), I_{\text{in}}(t')] = 0$ and similarly for I_{out} .¹⁸ The evaluation of $n^{(2)}$ thus proceeds in the following three steps: (i) We express $n(t)$ via the current operators using the general expression (3). (ii) We implement the normal-ordering for each term utilizing the prescription in terms of the *in-out*-ordering as explained above. (iii) In each term, we introduce the expression (5) for the current operators and then perform the average over the reservoir with the help of Wick's theorem for the electronic operators $c_{L/R}$. The relevant diagrams for calculating $n^{(2)}(\tau)$ are shown schematically in Fig. 3.

The photon-photon correlation function can be decomposed into two parts $n^{(2)}(\tau) = n_{\text{G}}^{(2)}(\tau) + n_{\text{nG}}^{(2)}(\tau)$ with a Gaussian term, which dominates at large temperatures

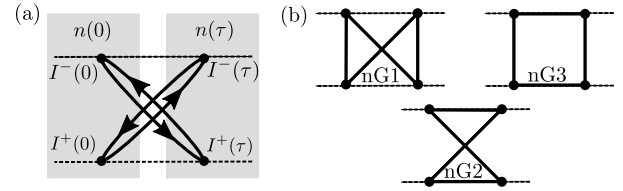


FIG. 3. Diagrams contributing to the photon-photon correlator $n^{(2)}$. The dashed lines denote the Keldysh contour and the current operators I^+ (I^-), denoted by black dots, are located on the lower (upper) branch. Each photon-number operator n (gray boxes) consists of a current operator on each branch. (a) The contribution due to Gaussian current-current fluctuations: Each current operator consists of two fermionic operators and the solid lines with the arrows indicate their contractions. Although the diagram is reducible in terms of the current operators [as it decays into a product of two second-order correlators $S(\omega)$], it contributes the genuine term (14) to the irreducible correlator $n^{(2)}(\tau)$. (b) The three diagrams (nG1, nG2, nG3) of the non-Gaussian contributions to the photon-correlation function that originate from irreducible forth-order current correlators. The sketches are analogous to (a): The current-operators are shown as black dots, the Keldysh contour as dashed lines, and the contractions as solid lines. We have omitted the arrows on the solid lines as each diagram contributes twice with the contributions differing by the direction of the arrows that define the contractions.¹⁹

and is always positive, given by

$$n_{\text{G}}^{(2)}(\tau) = \iint_0^\infty d\omega_1 d\omega_2 \alpha_{(\omega_1+\omega_2)/2}^2 |Z_{\omega_1}|^2 |Z_{\omega_2}|^2 \times S(\omega_1) S(\omega_2) \cos[(\omega_1 - \omega_2)\tau] \quad (14)$$

and a non-Gaussian term

$$n_{\text{nG}}^{(2)}(\tau) = \iint \frac{d\nu d\epsilon}{(2\pi)^2} \iint_{|\nu|/2}^\infty d\omega_1 d\omega_2 Z^{(2)}(\omega_1, \omega_2, \nu) \times (n_{\text{nG1}} + n_{\text{nG2}} + n_{\text{nG3}}) \cos(\nu\tau), \quad (15)$$

which depends through the combination

$$Z^{(2)} = \alpha_{\omega_1} \alpha_{\omega_2} \text{Re}(Z_{\omega_1-\nu/2} Z_{\omega_2+\nu/2} Z_{\omega_1+\nu/2}^* Z_{\omega_2-\nu/2}^*)$$

on the impedance Z_ω such that $n_{\text{nG}}^{(2)}$ different from $n_{\text{G}}^{(2)}$ depends on the phase of Z_ω . More importantly, the non-Gaussian term does not have a well-defined sign. In fact it has been shown that if the impedance is peaked in the frequency interval $[eV_0/2\hbar, eV_0/\hbar]$ and at low temperatures, the non-Gaussian contribution is negative and for proper choice of parameters even dominates the direct contribution.³

The non-Gaussian contribution involves the three diagrams nG1, nG2, and nG3. The general expressions are quite involved though they follow straightforwardly from the recipe outlined above. At zero temperature, only a few terms survive and the resulting contributions can be

written in the compact form

$$\begin{aligned}
n_{\text{nG1}} &= -2R^2T^2\Delta(\epsilon - \frac{1}{2}\nu)\Delta(\epsilon + \frac{1}{2}\nu)\Delta(\epsilon + \omega_1)\Delta(\epsilon + \omega_2), \\
n_{\text{nG2}} &= -2R^2T^2\Delta(\epsilon)\Delta(\epsilon + \omega_1 + \frac{1}{2}\nu)\Delta(\epsilon + \omega_2 + \frac{1}{2}\nu) \\
&\quad \times \Delta(\epsilon + \omega_1 + \omega_2), \\
n_{\text{nG3}} &= RT(1 - 2RT)\Delta(\epsilon)\Delta(\epsilon + \omega_2 - \frac{1}{2}\nu)\Delta(\epsilon + \omega_2 + \frac{1}{2}\nu) \\
&\quad \times \Delta(\epsilon + \omega_1 + \omega_2), \tag{16}
\end{aligned}$$

where $\Delta(\epsilon)$ selects electrons with energies ϵ within the transport window. In the following, we use the approximate expressions for $n_{\text{nG}j}$ also at finite temperatures. We have tested numerically that for low temperatures $\vartheta \lesssim eV_0/k_B$, which we are interested in, the results differ from the exact expression by not more than a few percent, see for example the dashed lines in Figs. 5 and 6. The analytical expressions in Eq. (16) are one of the central results of this paper as they provide an accurate analytical description of the physics which we want to discuss in the following.

From the three contributions, n_{nG1} and n_{nG2} are negative and thus lead to antibunching whereas n_{nG3} is positive. The three contributions have different physical origin. The first contribution n_{nG1} originates from a correlated emission of two photons at frequency ω_1 and ω_2 due to the transfer of two electrons. For $\nu = 0$, this term has already been discussed in Ref. 6. The other two terms are new and describe two photon processes where a single electron which is transmitted through the quantum point contact emits two photons. Note that these processes are suppressed for an environment such that the impedance for $\omega < eV_0/2\hbar$ is vanishingly small. In our setup, the smallness of the impedance in this regime is controlled by the quality factor Q .

The evaluation of $N^{(2)}$, which is needed for the Fano factor, involves the regime of long-measurement time. The integral over τ in (13) then reduces the number of frequency integrals in the expressions of $n^{(2)}(\tau)$ by one as $\int d\tau \cos(\nu\tau) = 2\pi\delta(\nu)$. Since the main negative contribution n_{nG1} to $n^{(2)}$ is largest for $T = \frac{1}{2}$, we will present only results for this case in the following.

V. ZERO TEMPERATURE

We first present the results at vanishing temperatures. In this case, the Fermi-Dirac distribution becomes a step function. The physics is concentrated on energies within the voltage bias with $\Delta(\epsilon) = 1$ for $\epsilon \in [0, eV_0]$ and zero otherwise. In the direct contribution to the photon-photon correlator, we can replace the shot-noise $S(\omega)$ by the zero temperature result $RT(\omega_0 - \omega)\Theta(\omega_0 - \omega)/2\pi$ and obtain

$$\begin{aligned}
n_{\text{G}}^{(2)}(\tau) &= \frac{R^2T^2}{4\pi^2} \iint_0^{\omega_0} d\omega_1 d\omega_2 (\omega_0 - \omega_1)(\omega_0 - \omega_2) \\
&\quad \times \alpha_{(\omega_1 + \omega_2)/2}^2 |Z_{\omega_1}|^2 |Z_{\omega_2}|^2 \cos[(\omega_1 - \omega_2)\tau] \tag{17}
\end{aligned}$$

Since $\Delta(\epsilon)$ is a step function, we can also simplify the expression for $n_{\text{nG}j}$ with the results

$$\begin{aligned}
n_{\text{nG1}} &= -2R^2T^2\Delta(\epsilon - \frac{1}{2}|\nu|)\Delta(\epsilon + \omega_1)\Delta(\epsilon + \omega_2), \\
n_{\text{nG2}} &= -2R^2T^2\Delta(\epsilon)\Delta(\epsilon + \omega_1 + \omega_2), \\
n_{\text{nG3}} &= RT(1 - 2RT)\Delta(\epsilon)\Delta(\epsilon + \omega_1 + \omega_2). \tag{18}
\end{aligned}$$

For $T = \frac{1}{2}$, which is the optimal choice to observe the photon antibunching, we have $n_{\text{nG2}} + n_{\text{nG3}} = 0$ and two photon processes are absent irrespective of the shape of $|Z_\omega|$. As, this feature will approximately persist also to some small but finite temperatures, the stringent requirements on the quality factor Q of the cavity can be relaxed. The ϵ integration can now be performed readily with the result (valid for $T = R = \frac{1}{2}$)

$$\begin{aligned}
n_{\text{nG}}^{(2)}(\tau) &= -\frac{2R^2T^2}{\pi^2} \int_{\mathcal{R}} d\nu d\omega_1 d\omega_2 (\omega_0 - \frac{1}{2}\nu - \omega_2) \\
&\quad \times Z^{(2)}(\omega_1, \omega_2, \nu) \cos(\nu\tau) \tag{19}
\end{aligned}$$

where the integration is constraint onto the region \mathcal{R} with $0 < \nu/2 < \omega_1 < \omega_2 < \omega_0 - \nu/2$.

The question whether the radiation can be classified as nonclassical relies on the competition between the positive (classical) contribution (17) and its negative counterpart (19). As explained before, for the evaluation of $N^{(2)}$ the cos-factor becomes a δ -function and thus reduces the number of integrals by one. Solving the remaining integrals yields the results (valid for $Q \gg 1$)

$$N_{\text{G}}^{(2)} = \pi^2 n_{\text{cav}}^2 \gamma, \quad N_{\text{nG}}^{(2)} = -8 \ln(2) \pi^2 n_{\text{cav}}^2 \gamma.$$

Because $|N_{\text{nG}}^{(2)}|/N_{\text{G}}^{(2)} = 8 \ln 2 \approx 5.5 > 1$ the Fano factor is below 1 and we obtain

$$F - 1 = \frac{(1 - 8 \ln 2) \pi^2 n_{\text{cav}}^2}{\ln(2Q)}, \quad Q \gg 1. \tag{20}$$

Next, we turn to the discussion of the photon-photon correlator. For $\tau = 0$, we obtain the result ($Q \gg 1$)

$$n_{\text{G}}^{(2)}(0) = n_{\text{cav}}^2 \gamma^2 \ln^2(2Q) \tag{21}$$

In the same limit of large quality factors, we can send the lower limit of integration in Eq. (17) to $-\infty$ as the integral is cut-off by the impedance. In this approximation, $n_{\text{G}}^{(2)}$ is independent of the applied voltage bias (which has been effectively sent to infinity). For large quality factors, the photon-photon correlations assumes the form

$$n_{\text{G}}^{(2)}(\tau) = n_{\text{cav}}^2 \gamma^2 \begin{cases} 16(\gamma\tau)^{-4}, & \gamma\tau \gg 1, \\ \ln^2(\gamma\tau), & \gamma\tau \ll 1. \end{cases} \tag{22}$$

This shows that the correlation time is given by γ . As we have neglected the finite value of the voltage, the results in (22) are only valid in the regime $Q^{-1} \lesssim \gamma\tau \lesssim Q$.

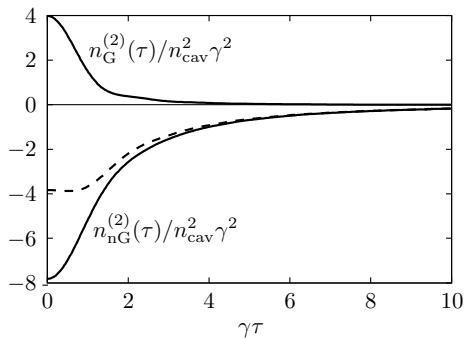


FIG. 4. Photon correlation functions $n_G^{(2)}(\tau)$ due to Gaussian current-current fluctuations and $n_{nG}^{(2)}(\tau)$ due to non-Gaussian fluctuations at zero temperature for $Q = 5$. It can be seen that both correlators decay on a characteristic scale set by the inverse of the cavity decay rate. The positive contribution $n_G^{(2)}$ and the negative contribution $n_{nG}^{(2)}$ add up to the photon-photon correlator $n^{(2)}(\tau)$ (dashed line). As $n^{(2)}$ is negative, the second-order coherence $g^{(2)}(\tau)$ is smaller than 1 indicating that the photons are antibunched.

Outside this regime, we have to include the finite value of $eV_0 = \hbar\omega_0$. For small times ($\gamma\tau < Q^{-1}$), the weak divergence for $\tau \rightarrow 0$ has to be cut-off at $\omega_0\tau \simeq 1$. For long times ($\gamma\tau > Q$), the photon-photon correlator shows an oscillatory component, cf. Fig. 4. The oscillatory part is approximately given by

$$n_G^{(2)}(\tau) = \frac{8n_{cav}^2[1 - \sin(eV_0\tau/\hbar)]}{\omega_0\tau^3}, \quad (23)$$

valid for $\omega_0\tau \gtrsim 1$. The reason for this oscillation lies in the fermionic statistics of the electrons producing the radiation. At low temperatures, due to the Pauli principle, the electrons contributing to the charge transport are separated by a time-interval \hbar/eV_0 that is a remnant of the exchange-hole found in a Fermi sea.^{20,21} The fact that electrons with the same spin are separated from each other leads to a separation of the photons which are produced by the electrons and correspondingly in a dip of the photon-photon correlator at the relevant timescale. Note that for long-times where the oscillatory behavior becomes visible, the photon-photon correlator is a factor Q^{-2} smaller than at $\tau = 0$ such that this oscillation although of theoretical interest will most likely remain experimentally unobservable.

We continue by discussing the competing negative contribution $n_{nG}^{(2)}$. For large quality factors $Q \gg 1$, the impedance $Z^{(2)}$ concentrates the integral (19) at values $\omega_{1/2} \simeq \omega_0$ and $\nu \simeq 0$. The value for $\tau = 0$ is approximately given by

$$n_{nG}^{(2)}(0) = -\frac{4\pi^2 n_{cav}^2 \gamma^2 \ln(Q)}{3}. \quad (24)$$

For finite times τ , we again proceed by sending the lower limit of integration to $-\infty$ which corresponds to integrat-

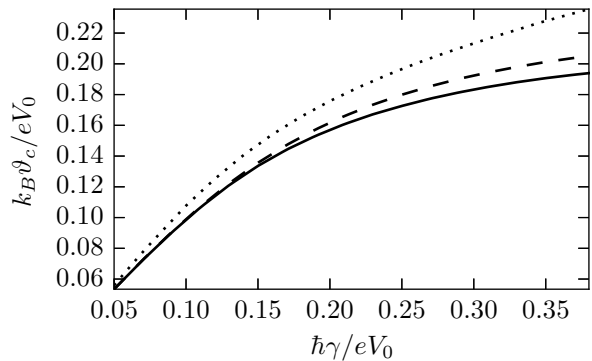


FIG. 5. Critical temperatures ϑ_c and ϑ_c^* as a function of the inverse quality factor $Q = \omega_0/\gamma = eV_0/\hbar\gamma$. The dashed line is the evaluation of ϑ_c with all terms contributing to the diagrams in Fig. 3(b) taken into account. This result should be compared to the solid line that involves the approximate expressions (16). The results differ by at most a few percent showing that (16) is a reasonable approximation for the relevant quality factors $Q \gtrsim 5$. Whereas ϑ_c indicates for which temperatures nonclassical signatures of the radiation can be detected in the time-averaged quantity (Fano factor), the dotted line shows the result for ϑ_c^* , the critical temperature for which the second-order coherence $g^{(2)}(\tau)$ is below 1. The latter is evaluated with the approximate expressions of Eq. (16).

ing over the region $\nu/2 < \omega_1 < \omega_2 < \omega_0 - \nu/2$. This approximation renders the result (valid for $Q \gtrsim \gamma\tau \gtrsim Q^{-1}$)

$$n_{nG}^{(2)}(\tau) = -\frac{2\pi^2 n_{cav}^2 \gamma^2}{3} \begin{cases} 3(\gamma\tau)^{-2}, & \gamma\tau \gg 1, \\ 2|\ln(\gamma\tau)|, & \gamma\tau \ll 1. \end{cases} \quad (25)$$

independent of the value of the bias voltage.

VI. CRITICAL TEMPERATURE FROM FANO FACTOR

On the one hand, we have seen that for a single channel wire and for large quality factors, the Fano factor is below 1 at zero temperature, cf. Eq. (20). On the other hand, for large temperatures $k_B\vartheta \gg eV_0$, the Fano factor approaches $F = 1 + n_{cav} > 1$, characteristic for a thermal source. Thus, there is some critical temperature ϑ_c at which the Fano factor is 1. In the time-averaged quantities, the nonclassical signatures of the radiation source thus is only visible for $\vartheta < \vartheta_c$. Figure 5 shows the result for ϑ_c as a function of the inverse quality factor. For $Q \geq 10$, the critical temperature is well-approximated by $\vartheta_c \approx \hbar\gamma/k_B$. Note that the fact that the critical temperature scales with the photon-loss rate γ has already been noted in Ref. 6. For $Q = 5$, we have approximately $\vartheta_c \approx 0.16 eV_0/k_B$.

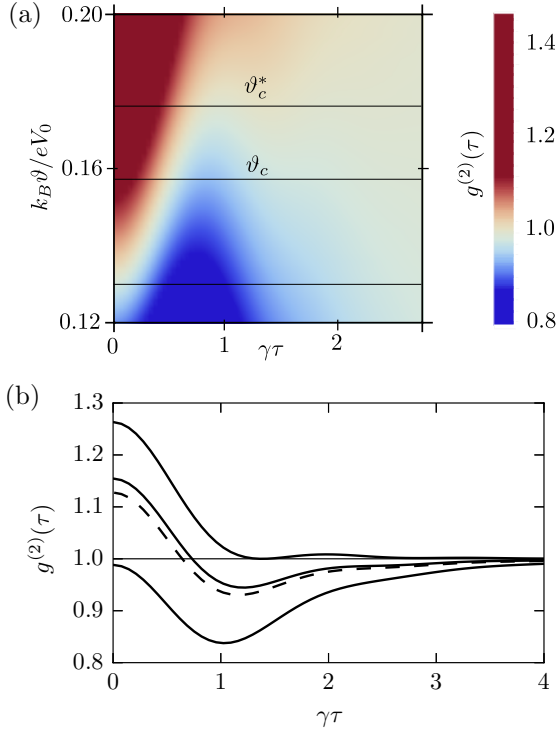


FIG. 6. (a) (color online) The second-order coherence $g^{(2)}(\tau)$ as a function of the autocorrelation time τ and the temperature ϑ of the electronic system. The data have been evaluated for a quality factor $Q = 5$ using the approximate expressions (16). (b) Line cuts (solid lines) for temperatures ϑ_c^* , ϑ_c , and $\vartheta = 0.13 eV_0/k_B$ from top to bottom. The dashed line is a calculation for $\vartheta = \vartheta_c$ using the exact expression for the diagrams in Fig. 3(b). It can be seen that the approximation (16) captures all essential features and even underestimates the nonclassical correlations.

VII. CRITICAL TEMPERATURE FROM SECOND-ORDER COHERENCE

Knowing the critical temperature, we have confirmed numerically that the following approximations holds at low temperatures: $n_G^{(2)}$ remains largely unchanged with temperature whereas $n_{nG}^{(2)}$ scales with a factor $(1 - 0.6\vartheta/\vartheta_c)$. As a result, we have the approximate expression

$$n^{(2)}(\tau) = n_G^{(2)}(\tau; \vartheta=0) + \left(1 - \frac{0.6\vartheta}{\vartheta_c}\right) n_{nG}^{(2)}(\tau; \vartheta=0) \quad (26)$$

for the photon-photon correlator at finite temperatures. In Fig. 4, we can see that $n_G^{(2)}(\tau; \vartheta=0)$ falls off fast for small times when compared to $n_{nG}^{(2)}(\tau; \vartheta=0)$. We can understand this from the analytical expressions in Sec. V by comparing the behavior of $\ln^2|\gamma\tau|$ for $n_G^{(2)}$ to $\ln|\gamma\tau|$ for $n_{nG}^{(2)}$. Starting from a finite value at $\tau = 0$, $n_G^{(2)}$ has a point of inflection just before going over to the $\ln^2|\gamma\tau|$ behavior. Numerically, we obtain a value $\tau^* \approx 5\omega_0^{-1}$ for the position of this point. Due to the

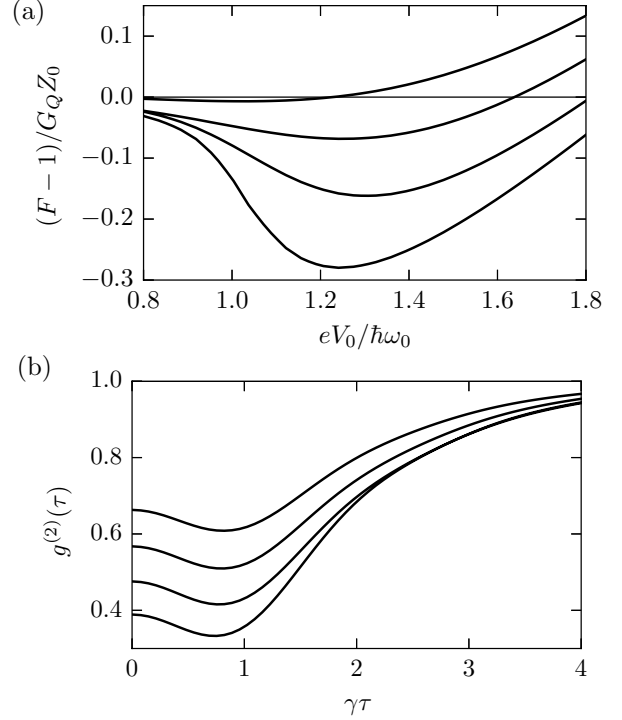


FIG. 7. (a) The plot shows the Fano factor F as a function of V_0 for temperatures $\vartheta = (0, 0.05, 0.1, 0.15)\hbar\omega_0/k_B$ from bottom to top. It can be seen that at low temperatures the minimal value of F is achieved slightly above the resonant condition with $eV_0 \approx (1.2-1.3)\hbar\omega_0$. (b) Second-order coherence $g^{(2)}(\tau)$ for the temperature $\vartheta = 0.05\hbar\omega_0/k_B$ as a function of τ . The different lines correspond to different bias voltages with $V_0 = (1.0, 1.1, 1.2, 1.3)\hbar\omega_0/e$ from bottom to top. The second-order coherence offers additional time-resolved information when compared to the Fano factor. For finite temperatures, $g^{(2)}$ is a nonmonotonous function with a minimum at time $\tau^* \approx 5\omega_0^{-1}$. All the results have been obtained using the realistic value $Q = \omega_0/\gamma = 5$ for the quality factor.

fast decay of $n_G^{(2)}$ and the fact that the contribution of $n_{nG}^{(2)}$ is reduced at finite temperatures, the second-order coherence $g^{(2)}(\tau)$ becomes nonmonotonous at finite temperature with a well-pronounced minimum slightly above τ^* , see Fig. 6. Due to the oscillatory behavior, we expect to obtain $g^{(2)}(\tau \approx \tau^*) < 1$ at temperatures above ϑ_c . We denote with ϑ_c^* the critical temperature below which $g^{(2)}(\tau^*) < 1$. The critical temperature is shown as the dotted line in Fig. 5. Indeed, for relevant quality factors $Q < 10$, ϑ_c^* is about 10% larger than ϑ_c rendering the requirements to see nonclassical correlation less stringent.

VIII. EXPERIMENTAL PARAMETERS

In this section, we would like to present realistic experimental parameters to observe sub-Poissonian statistics ($F < 1$) of the radiation emitted by the quantum

point contact. As can be seen in Fig. 5, the critical temperature increases with decreasing quality factor. It flattens out for $\hbar\gamma/eV_0 = 0.2$. However, the results have assumed the impedance of the transmission line to be constant over the range set by γ . Thus, a quality factor of $Q = 5$ seems to offer an appropriate balance between having a large critical temperature while still only requiring a moderate bandwidth for the detector. Since the results of this paper rely on having a single electronic channel without spin-degeneracy, a point contact in a quantum Hall edge channel in a sufficiently large magnetic field is essential. The constricting has to be tuned to a transparency of $T = \frac{1}{2}$. It is reasonable to expect that the conductance remains linear for voltages up to $V_0 = 100 \mu\text{V}$. In order to optimize the Fano factor, we propose $eV_0/\hbar\omega_0 = 1.3$ such that $\omega_0 \approx 2\pi \times 18 \text{ GHz}$. In order to achieve $k_B\vartheta/\hbar\omega_0 = 0.05$, an electronic temperature of the order of $\vartheta \approx 50 \text{ mK}$ has to be obtained. From Fig. 7, we can then see that in this case the Fano factor reads $F = 1 - 0.15G_QZ_0$. The possibility to observe the sub-Poissonian nature of the radiation in the end relies on the impedance matching of the transmission line to the quantum point contact that is captured in the expression G_QZ_0 . For example, if the sensitivity allows to distinguish $F = 1$ from $F = 0.95$, an impedance matching with $G_QZ_0 = 0.33$ ($Z_0 \approx 8 \text{ k}\Omega$) is required.

IX. CONCLUSIONS

In conclusion, we have calculated the second-order coherence of microwave radiation produced by a quantum point contact with a single transport channel. We have obtained the approximate analytical expression Eq. (16) that provides accurate results for the relevant temperatures where the radiation is nonclassical. We have shown that at low temperatures and at transparency $T = \frac{1}{2}$, two photon processes are suppressed due to the cancellation of two competing terms. As a result, the stringent requirements on the quality factor of the LC -resonator can be relaxed which helps to increase the measurement signal. We have given explicit analytical results for the photon-photon correlators at zero temperature and an approximate expression valid at finite but small temperatures. We have shown that the second-order coherence $g^{(2)}(\tau)$ shows a nonmonotonous behavior with a minimum close to $\tau^* \approx 5\omega_0^{-1}$. Taking the minimum of $g^{(2)}$ as the criterion for nonclassical radiation, the critical temperature below which nonclassical features can be observed is increased by 10% compared to time-averaged quantities. We have presented a set of realistic though challenging experimental parameters that allow for the detection of the sub-Poissonian radiation emitted by the quantum point contact.

ACKNOWLEDGMENTS

The authors thank Fabien Portier for fruitful discussions and for providing the motivation for this research. They acknowledge financial support via the Alexander von Humboldt-Stiftung.

¹ E. M. Purcell, The question of correlation between photons in coherent light rays, *Nature* **178**, 1449 (1956).

² B. Lounis and M. Orrit, Single-photon sources, *Rep. Prog. Phys.* **68**, 1129 (2005).

³ C. W. J. Beenakker and H. Schomerus, Antibunched photons emitted by a quantum point contact out of equilibrium, *Phys. Rev. Lett.* **93**, 096801 (2004).

⁴ C. W. J. Beenakker and H. Schomerus, Counting statistics of photons produced by electronic shot noise, *Phys. Rev. Lett.* **86**, 700 (2001).

⁵ A. V. Lebedev, G. B. Lesovik, and G. Blatter, Statistics of radiation emitted from a quantum point contact, *Phys. Rev. B* **81**, 155421 (2010).

⁶ I. C. Fulga, F. Hassler, and C. W. J. Beenakker, Nonzero temperature effects on antibunched photons emitted by a quantum point contact out of equilibrium, *Phys. Rev. B* **81**, 115331 (2010).

⁷ G. B. Lesovik and R. Loosen, On the detection of finite-frequency current fluctuations, *JETP Lett.* **65**, 295 (1997).

⁸ E. Zakka-Bajjani, J. Ségala, F. Portier, P. Roche, C. Glattli, A. Cavanna, and Y. Jin, Experimental test of the high-frequency quantum shot noise theory in a quantum point contact, *Phys. Rev. Lett.* **99**, 236803 (2007).

⁹ E. Zakka-Bajjani, J. Dufouleur, N. Coulombel, P. Roche, D. C. Glattli, and F. Portier, Experimental determination of the statistics of photons emitted by a tunnel junction, *Phys. Rev. Lett.* **104**, 206802 (2010).

¹⁰ M. Hofheinz, F. Portier, Q. Baudouin, P. Joyez, D. Vion, P. Bertet, P. Roche, and D. Esteve, The bright side of Coulomb blockade, *Phys. Rev. Lett.* **106**, 217005 (2011).

¹¹ C. Altimiras, O. Parlavecchio, P. Joyez, D. Vion, P. Roche, D. Esteve, and F. Portier, Tunable microwave impedance matching to a high impedance source using a Josephson metamaterial, *Appl. Phys. Lett.* **103**, 212601 (2013).

¹² When including N -channels, it turns out that the positive (Gaussian) contribution $n_G^{(2)}$ to $n^{(2)}$ is proportional to N^2 , whereas the negative (non-Gaussian) contribution $n_{\text{nG}}^{(2)}$ only grows like N .

¹³ G.-L. Ingold and Yu. V. Nazarov, Charge tunneling rates in ultrasmall junctions, in *Single Charge Tunneling*, edited

- by H. Grabert and M. H. Devoret, vol. 294 of *NATO ASI Series B*, pp. 21–107 (Plenum Press, New York, 1992).
- ¹⁴ C. Padurariu, F. Hassler, and Yu. V. Nazarov, Statistics of radiation at Josephson parametric resonance, *Phys. Rev. B* **86**, 054514 (2012).
- ¹⁵ Note that the combination $\alpha_\omega |Z_\omega|^2 / 2\pi$ corresponds to $\gamma(\omega)$ of Ref. 3.
- ¹⁶ In the solid-state community this is also known as Keldysh ordering with ‘ \pm ’ being the label for the Keldysh contour.
- ¹⁷ C. Emary, C. Pörtl, A. Carmele, J. Kabuss, A. Knorr, and T. Brandes, Bunching and antibunching in electronic transport, *Phys. Rev. B* **85**, 165417 (2012).
- ¹⁸ The equivalence of these two orderings has been the source of some controversy. The equivalence has been recently shown rigorously in Refs. 22. The equivalence relies on the fact that the scattering matrix is strictly causal as expected for a realistic system. In the case of an energy independent scattering matrix as treated here, the strict causality is lost and the time-ordering has to be replaced by Matthews’ T^* time-ordering.
- ¹⁹ More information about the calculation of the current-current correlators can be found in D. Otten, masters thesis, RWTH Aachen University, 2015.
- ²⁰ Th. Martin and R. Landauer, Wave-packet approach to noise in multichannel mesoscopic systems, *Phys. Rev. B* **45**, 1742 (1992).
- ²¹ F. Hassler, M. V. Suslov, G. M. Graf, M. V. Lebedev, G. B. Lesovik, and G. Blatter, Wave-packet formalism of full counting statistics, *Phys. Rev. B* **78**, 165330 (2008).
- ²² S. Bachmann, G. M. Graf, and G. B. Lesovik, Time ordering and counting statistics, *J. Stat. Phys.* **138**, 333 (2010). V. Beaud, G. M. Graf, A. V. Lebedev, and G. B. Lesovik, Statistics of charge transport and modified time ordering, *ibid.* **153**, 177 (2013).